Journal of Pharmaceutical Research International

33(42B): 102-123, 2021; Article no.JPRI.73307
ISSN: 2456-9119
(Past name: British Journal of Pharmaceutical Research, Past ISSN: 2231-2919, NLM ID: 101631759)

Formulation and Evaluation of Miconazole Nitrate Loaded Nanoparticles for Topical Delivery

Ashish Y. Pawar[1*], Khanderao R. Jadhav[2], Komal D. Ahire[1] and Tushar P. Mahajan[1]

[1]Department of Pharmaceutics, MGV's Pharmacy College, Panchavati, Nashik, Maharashtra State, 422 003, India.
[2]Department of Pharmaceutics, Divine College of Pharmacy, Satana, Dist. Nashik, Maharashtra State, 423 301, India.

Authors' contributions

This work was carried out in collaboration among all authors. All authors read and approved the final manuscript.

Article Information

DOI: 10.9734/JPRI/2021/v33i42B32432
Editor(s):
(1) Dr. Syed A. A. Rizvi, Nova Southeastern University, USA.
Reviewers:
(1) Tenderwealth Clement Jackson, University of Uyo, Nigeria.
(2) Omali Yousef Elkhawaga, Mansoura University, Egypt.
Complete Peer review History: https://www.sdiarticle4.com/review-history/73307

Original Research Article

Received 20 June 2021
Accepted 26 August 2021
Published 31 August 2021

ABSTRACT

The aim of the present work was to formulate and evaluate Miconazole nitrate (MN) polymeric nanoparticles (NPs) for systemic delivery of the active ingredient after topical administration. The Solvent evaporation approach was used to make nanoparticles for topical delivery of MN. Particle size, entrapment efficiency and SEM were all measured in MN-SLN. A consistent size distribution (PI 0.300) was used to generate aqueous NPs dispersions with a mean particle size less than 250 nm. After 3 months of storage, the produced semi-solid systems had a mean particle size of less than 250 nm and a PI of less than 0.500. The F5 formulation was been chosen as the model formulation from among the nine nanoparticle formulations developed (F1 to F9). The reason for this was that, according to the ICH stability guidelines, formulation F5 was judged to be optimal and stable. The F5 formulations of miconazole nanoparticles shows the highest entrapment efficiency (93.28%) and drug loading (86.64%). In conclusion, there are two major advantages of using miconazole nanoparticle drug delivery systems. i.e., they are topical preparations that assemble in the hair follicles and wrinkles to produce a systemic and local action. It is possible that nanoparticles will be the most effective treatment for fungal skin infections.

**Corresponding author: E-mail: pawarashish23@gmail.com;*

Keywords: Chitosan; nanoparticle; miconazole; anti-fungal; topical.

1. INTRODUCTION

Nanotechnology is a rapidly developing field that involves the creation and use of nano-sized particles that are measured in nanometers. In other words, nanotechnology is the science, engineering, technology, drug delivery, and therapies revolutionized by the art of characterizing, manipulating, and organizing matter systemically at the nanoscale scale. The size of typical accessible structures is in the sub-micrometer range, which is beyond the optical resolution of a light microscope and hardly visible. This scale is around 1/1000 the size of structures visible to the human eye, but 1000 times the size of an atom. Because a common structural size is in the nanoscale range, recent discoveries are addressing the size range below these dimensions, and the methods and techniques are referred to as nanotechnology [1].

There are several traditional therapies and treatment methods available which are time consuming and very expensive. With the nanotechnology, treatments can be developed significantly faster and for a reasonable cost using nanotechnology in the pharmaceutical area. Another advantage of pharmaceutical nanotechnology is that it can be used in a variety of ways. Normally, medications work their way through the entire body before reaching the diseased location. The drug can be targeted to a specific location using nanotechnology drugs, making it far more effective and reducing the risk of negative effects [2]. Pharmaceutical Nanotechnology offers a unique and comprehensive approach to cancer treatment, including early detection, prediction, prevention, individualized therapy, and medication. Priority research areas in which nanotechnology would play a vital role include target-specific drug therapy and methods for early diagnosis of pathologies [3].

1.1 Nanoparticle

A nanoparticle, also known as an ultrafine particle, is a small particle of matter with a dimension of 1 to 100 nanometres (nm). [4,5] The phrase is also applied to bigger particles of up to 500 nm in diameter, as well as fibers and tubes with a diameter of less than 100 nm in only two dimensions [6]. Metal particles less than 1 nm are commonly referred to as atom clusters instead. Nanoparticles are distinguished from microparticles (1-1000 m), "fine particles" (sized between 100 and 2500 nm), and "coarse particles" (sized between 2500 and 10,000 nm) by their smaller size, which influences very different physical and chemical properties, such as colloidal properties and optical or electric properties [7].

They do not sediment as much as colloidal particles because they are more prone to brownian motion. Colloidal particles, on the other hand, are commonly thought to vary from 1 to 1000 nm. Nanoparticles cannot be detected with standard optical microscopes because their wavelengths are substantially shorter than visible light wavelengths (400-700 nm), necessitating the use of electron microscopes or laser microscopes. Dispersions of nanoparticles in transparent liquids can be transparent for the same reason, although suspensions of bigger particles reflect some or all visible light striking on them. Nanoparticles also flow through conventional filters, such as common ceramic candles [8], therefore separation from liquids necessitates the use of specialized equipment.

Nanoparticles have features that differ significantly from larger particles of the same substance. Because an atom's diameter is typically between 0.15 and 0.6 nm, a major portion of the nanoparticle's substance is found within a few atomic diameters of its surface. As a result, the top layer's properties may take precedence over those of the bulk material. Because the interactions between the two materials at their interface become considerable, this effect is especially powerful for nanoparticles distributed in a liquid of dissimilar composition [9]. Individual atoms are shown in this idealized picture of a crystalline platinum nanoparticle with a diameter of roughly 2 nm.

Nanoparticles are found all throughout nature and are studied in a variety of fields including chemistry, physics, geology, and biology. They frequently display behaviors that are not observed at either size because they are at the interface between bulk materials and atomic or molecular structures. They are a major source of pollution in the atmosphere and are used in a variety of industrialized products such as paints, plastics, metals, ceramics, and magnetic objects. Nanotechnology's manufacture of nanoparticles with specialized characteristics is an important branch. Nanoparticles, in general, have a smaller

concentration of point defects than their bulk counterparts [10], but they do sustain a variety of dislocations that can be seen with high-resolution electron microscopes [11]. Nanoparticles, on the other hand, have different dislocation mechanics than bulk materials, which, when combined with their distinctive surface structures, results in mechanical properties that are distinct from the bulk material [12,13,14].

Infections caused by fungi are a widespread medical problem around the world. Candidiasis, congenital candidiasis, intertrigo, dermatitis, and dermatophytosis are examples of these infections. Many fungal diseases are treated with oral or parenteral medications, with topical preparations available in limited quantities [15]. Similarly, nanoparticles are presently being developed and tested for oral and parenteral delivery, with just a small amount of research done on topical administration. The goal of nanoparticle-based drug delivery systems is to transport medications to a specific place in the body, which is a difficult undertaking. As a result, many strategies for site-specific targeting of these medicines have been published in the literature to address these difficulties. The small size and huge surface area of these nanoparticulate systems enhance absorption at the cellular level, which is a key benefit [15-18].

2. MATERIALS

Miconazole nitrate was obtained from GlaxoSmithKline Pharmaceuticals Ltd, Ambad, Nashik. Chitosan was gotten from Modern Science, Nashik. Dichloromethane was obtained from modern Science, Nashik Ambad, Nashik. Polyvinylalcohol was obtained from Modern Science, Nashik.

3. MATERIALS AND METHOD

3.1 Organoleptic Characterization of Drug

Organoleptic characterization of Miconazole Nitrate was done by studying color, odor and appearance.

3.2 Melting Point

The melting factor (m.p.) is the temperature at which a stable with solid converts into Liquid [16,18]. The melting factor of Miconazole Nitrate changed into studied by thiele tube method.

3.3 Solubility

The Solubility of Drug in Water, methanol, Ethanol and 6.8 Buffer solutions was determined by Shake Flask technique. The tested Compound became dissolved in stable extra in 1-10 ml respective solvent. The answers had been stirred for forty eight hours within the magnetic stirrer beneath thermostated instances till the solubility equilibrium. to separate stages the answers were left to sediment below thermostate occasions. the solution turned into filtered. Aliquotes were taken from clean part of the solution. The aliquotes had been diluted the absorption changed into measured with UV-Spectrophotometer Shimadzu, UV-2450. The concentrations of the Aliquotes have been calculated [19].

3.4 U. V. Spectrum

The Miconazole Nitrate become subjected to UV spectroscopic analysis (Shimadzu; UV 2450) to find out the wavelength (λmax) at which it suggests most absorbance. Drug became accurately weighed and dissolved in solvent Methanol to obtain stock solution of 1000µg/ml. This answer become then definitely diluted with same solvent to get answer of awareness one 100 µg/ml. Then the UV spectrum of this concentration turned into recorded over the wavelength range 200-400 nm. The UV spectrum of drug was also taken in solvent Methanol and 6.8 PBS [20,21].

3.5 Determination of Maxima Absorbance (λ Max)

Stock solution (100µg/ml) of Miconazole Nitrate was prepared in methanol, pH 6.8 phosphate buffer, separately. This solution was then diluted using respective solvent to obtained suitable concentration. The UV spectrum was recorded in the range of 200-400 nm by using UV double beam spectrophotometer (Shimadzu2450). The wavelength of maximum absorption was determined [16,17,21].

1) Calibration curve of Miconazole Nitrate in Methanol

Parameters for the calibration curve of Miconazole Nitrate are shown in Table 1.

Table 1. Parameters for Calibration curve of Miconazole Nitrate in Methanol

Sr. No.	Parameter	Inference
1	Drug	Miconazole Nitrate
2	Conc. of stock solution	100 µg/ml
3	Absorption Maximum	271. 72 nm
4	Solvent	Methanol
5	Scanning Range	400-200 nm
6	Instrument	Shimadzu 2450
7	Sample Holder	Quartz

In this method weighed accurately 10 mg of Miconazole Nitrate and transferred to 100 ml volumetric flask .The drug was dissolved in methanol and made up the volume and sonicated for 5 min. This was used as the standard stock solution for further dilutions. Appropriate quantities of aliquots (1 ml) of the standard stock solution were taken in 10 ml volumetric flask .These were then diluted and made volume with methanol to made 2, 4, 6, 8, 10 and 12 µg/ml concentrations. The above solution were analyzed by UV spectrometer at λ max 271. 72 nm methanol was used as a blank during spectrophotometric analysis [20,22].

2) Calibration curve in 6.8 pH phosphate buffer

a. Preparation of 6.8 pH phosphate buffer

The 0.2M of KH_2PO4 solution was prepared by dissolving 2.722 gm of KH_2PO4 in 100 ml DW. In another 100 ml of volumetric flask, solution of 0.2 M NaOH was prepared by dissolving 0.8 gm NaOH in 100 ml DW. 50 ml of 0.2M KH_2PO4 solution was taken in another beaker and specified volume of 0.2N NaOH solution (22.4 ml) was added in it and the volume was adjusted with DW to 200 ml.

b. Standard stock solution

In this method 10 mg of drug was accurately weighed and transferred to calibrated 100 ml volumetric flask. It was dissolved in 6.8 pH phosphate buffer and volume was made up to 10 ml with same solvent to obtain a final concentration of 100µg/ml.

c. Working stock solution

This was used as the standard stock solution for further dilutions. Appropriate quantities of aliquots (1 ml) of the standard stock solution were taken in 10 ml volumetric flask. These were then diluted and made volume with 6.8 PBS to made 5, 10, 15, 20, 25 ug/ml were analyzed by UV-Visible spectrophotometer at λ max 272 nm. 6.8 PBS used as blank during spectrophotometric analysis. The standard calibration curve was obtained & plotting absorbance vs. concentration.

3.6 FTIR Spectrum

The dry sample of Drug was mixed with KBr in the ratio of 1: 9. The sample was triturated and finally placed in sample holder. The spectrum was scanned over frequency range 4000-400cm-1 in FTIR instrument Shimadzu IRAffinity-1S. The spectral analysis was done, by standard absorbance of the functional groups [23].

3.7 Differential Scanning Calorimetry (DSC) Studies

The DSC analysis of drug sample of Miconazole Nitrate was performed using DSC instrument (Shimadzu, DSC 60). Small amount of Miconazole Nitrate (2 to 3 mg) was accurately balanced in aluminum pan, hermetically sealed with the help of crimper and sample pan and reference pan are kept in DSC analyzer than Sample was heated from ambient temperature 40^0C to 400^0C, with the heating rate of 10^0C/min. Inert atmospheres was provided by purging nitrogen gas flowing at 100 ml/min [23].

3.8 Drug-Polymers compatibility studies

The preliminary compatibility was carried out using FTIR Spectrometer Schimadzu IRaffinity-1s.

3.9 FTIR Spectroscopy

The FTIR spectrum was recorded from 4500cm-1. Infrared spectra of pure Drug and physical mixture of Drug with polymers were obtained by using Standard KBr sample. A compatibility study for Miconazole Nitrate was carried out. Excipients studied included Chitosan, physical mixture. This sample was subjected to compatibility studies and stored for 30 days at elevated temperature and humidity conditions of 40 ± 20 C / 75 ± 5 % RH. After 30 days, IR spectra of this stored sample was obtained. IR studies of the drug and excipient was carried out to understand the compatibility between them [24,25].

4. FORMULATION OF MICONAZOLE NITRATE NANOPARTICLE

4.1 Formulation of Miconazole Nitrate Loaded Nanoparticle by Emulsification / Solvent Evaporation Method

The nanoparticles were made using the emulsification / solvent evaporation process. Miconazole Nitrate and Chitosan were dissolved in different quantities in Dichloromethane (DCM). High-energy shearing with a probe Sonicator (Athena Technology) at 50 percent amplitude for 10 minutes reduced the size of the globules in the emulsion, followed by the addition of 10 mL 2 percent Polyvinyl alcohol (PVA). For the isolation of dry NPs, the NPs dispersion was centrifuged at 15,000 RCF for 30 minutes using (REMI equipment) after overnight evaporation of DCM. The pellet was dispersed in de-ionized water before being freeze-dried with a (Vir Tis bencbtop K) freeze drier [23].

4.2 Optimization of Formulation

Miconazole nitrate loaded NPs were optimised using a 3^2 randomized full factorial design. The design was used to investigate the effect of Chitosan and DCM concentrations on formulation. In this study, the amounts of Chitosan (x1) and DCM (x2) were chosen as independent variables. These two variables were rated on three levels: higher, middle, and lower, with coding +1, 0 and -1, respectively. X1 levels of 5, 75, and 100 mg were chosen, whereas X2 levels of 2, 4, and 6 ml were chosen. Entrapment efficiency (Y1) and particle size were the dependent or response variables (Y2) [23-28]. Optimization formula shows in Table 2.

5. CHARACTERIZATION AND EVALUATION OF FORMULATED BATCHES OF PREPARED NANOPARTICLES

a) Physical appearance

Physical appearance of prepared NPs was observed visually. The white powder was observed.

b) Drug entrapment efficiency

At 272 nm, the percentage of Miconazole incorporated (entrapment efficiency) was evaluated spectrophotometrically. The amount of free drug was identified in the supernatant after centrifugation of the aqueous mixture, and the amount of integrated drug was calculated as the result of the initial drug minus the free drug [26].

Table 2. Composition of different batches of Miconazole loaded NPs

Formulation Code	Miconazole (mg)	Chitosan (mg) (X1)	DCM (ml) (X2)	PVA(2%) (ml)
F1	25	50	2	10
F2	25	50	4	10
F3	25	50	6	10
F4	25	75	2	10
F5	25	75	4	10
F6	25	75	6	10
F7	25	100	2	10
F8	25	100	4	10
F9	25	100	6	10

The following formula can be used to calculate entrapment efficiency:

$$EE = \frac{W\text{ (initial drug) - W (free drug)} \times 100}{W\text{ (initial drug)}}$$

c) Production yield:

The production yield was calculated using the formula below [29]. The results are given in Table 18.

$$\text{Production yield} = \frac{\text{(Practical yield)}}{\text{(Theoretical yield)}} \times 100$$

d) Particle size determination

Malvern Zetasizer measured the average particle size and size distribution of nanoparticles at room temperature. Before the measurement, the batch was diluted with double-distilled filtered water to achieve the proper particle concentration to avoid polydispersity events. The colloidal mixture (NP) is added to the sample dispersion unit under gentle agitation to minimize particle aggregation caused by particle-to-particle interactions. According to the particle size, the polymer and crosslinking agent showing the smallest particle size are selected for further preparation [26].

6. OPTIMIZED FORMULATION BATCH SELECTION

Optimized batch was selected as per the finding obtained during optimization. The batch shows least particle size with maximum entrapment efficiency will be considered. The nanoparticles were formulated using same composition as per solutions. The optimized batch were selected on the basis of experimental and predicted value were critically compared and prediction error calculated [27,30].

6.1 Lyophilization

Developed formulation were converted into dry powder using lyophilization technique. The effect of cryoprotecting agent such as sucrose, mannitol, lactose, ß-cyclodextrin, fructose, trehalose, dextrose and pearlitol on the stability of nanoparticles was studied. In 5ml of formulation, this cryoprotectants were added in increasing concentration 3%, 5%, 7% (concentration selected as per literature survey) and lyophilized for 24h at - 50°C temperature and 0.011 mbar pressure. The lyophilized nanoparticles were reconstituted in double distilled water and analyzed for particle size [23].

7. EVALUATION AND CHARACTERIZATION OF OPTIMIZES BATCH OF MICONAZOLE NITRATE LOADED NANOPARTICLES

7.1 Micromeritics Parameter of Prepared NP's

a) Bulk density: The NPs were carefully poured into a graduated cylinder after being precisely weighed. The NPs were then made uniform without disturbing them after pouring them into the graded cylinder. The volume was then determined by using a measuring cylinder with graduation marks labelled in millilitres. The observed volume was referred to as the bulk volume, and it was computed using the formula below.

$$\text{Bulk density} = \frac{\text{Mass of sample in gram}}{\text{Volume occupied by sample}}$$

b) Tapped density:

The measuring cylinder, which contained a known weight of NPs, was tapped for a predetermined amount of time. The powder was weighed and the cylinder's minimum volume was measured. The formula was used to compute the tapped density.

$$\text{Tapped density} = \frac{\text{Mass of sample (gm)}}{\text{Volume occupied by sample (ml)}}$$

c) Hausner's ratio:

It's a number that's linked to the flowability of powdered materials. The following formula is used to compute Hausner's ratio.

$$\textbf{Hausner's ratio} = \frac{\text{Tapped density}}{\text{Bulk density}}$$

A similar index has been defined by Hausner's ratio, standard value of Hausners ratio shown in Table 3.

d) Carr's Index:

The percent compressibility C, which is defined as follows, is an important measure that can be determined from bulk density determinations .Standard value of C.I. shown in Table 4.

$$\text{Carr's Index} = \frac{\text{Tapped density - Bulk density} \times 100}{\text{Tapped density}}$$

e) Angle of repose:

The powder blend's angle of repose was determined using the funnel method. A funnel was used to collect the properly weighed powder. The height of the funnel was adjusted such that the tip of the funnel just brushed the summit of the powder heap. The powder cone's diameter was measured, and the angle of repose was computed using the equation below. The results are given in Table 5.

$$\tan \theta = h/r$$

Where

r and h are the radius and height of the powder cone respectively.

7.2 FTIR

In the wavelength region of 4000 to 400 cm-1, the FTIR spectra of Miconazole Nitrate loaded Nanoparticles formulation batch was acquired. Miconazole nitrate's unique IR absorption peaks.

7.3 Determination of Drug Loading

The Miconazole Nitrate loaded Nanoparticles were weighed at ten milligrammes and dissolved in ten millilitres of methanol, centrifuged, filtered, and the filtrate measured at 272 nm using UV-Visible spectrophotometry. The experiment was repeated three times, and the drug loading was determined using the equation [26,31].

$$\text{Drug loading} = \frac{\text{Weight of drug loaded in NP} \times 100}{\text{Weight of nanoparticle}}$$

7.4 Particle Size and PDI Value

The mean particle size analysis and PDI value was done with the help of Malvern zetasizer to evaluate the effect of concentration of polymer on size [26].

7.5 Zeta Potential

Zeta potential determines stability of formulation by measuring change of the drug loaded droplet surface. Zeta potential for optimized batch was measured using Malvern Zetasizer, (particulate system) [26].

The zeta potential values were calculated using the smoluchwski equation.

7.6 Scanning Electron Microscopy (SEM)

Scanning electron microscopy was used to examine the shape and surface morphology of Miconazole-loaded NP. SEM analysis was performed using ZEISS, Japan, and the sample was coated with gold ion for 5-6 minutes before being studied at 1,000 and 1,500X magnification [26].

7.7 Differential Scanning Calorimetry

To characterise the physical condition of prepared Miconazole Nitrate loaded NPs, DSC was used. Approximately 3-4 mg of produced NPs were weighed, crimped into an aluminium pan, and examined at a scanning temperature of 500 C to 4000 C at a heating rate of 100 C/min [30].

8. RESULTS AND DISCUSSION

8.1 Preformulation Studies

8.1.1 Organoleptic properties

The organoleptic characteristics of the drug sample received were examined, including colour, odour, and appearance. The results are reported in Table 6.

8.1.2 Melting Point

Melting point of Miconazole nitrate is given in Table 7. The melting point of drug is within the range of values in official books that indicates the gift sample obtained are of pure.

8.1.3 Solubility

The drug Miconazole nitrate was shown to be practically insoluble in distilled water, with solubilities of 2.9, 11.9, and 11.15 in ethanol, methanol, and phosphate buffer pH 6.8 correspondingly. It means the drug is weakly

soluble in ethanol, sparingly soluble in methanol, and hardly soluble in phosphate buffer at pH 6.8.The solubility of miconazole in different solvent shown in Table 8.

8.1.4 Ultraviolet-Visible spectroscopy study

8.1.4.1 Determination of λ_{max} of Miconazole nitrate in methanol and 6.8 phosphate buffer

The UV spectrum of Miconazole nitrate solution in methanol and phosphate buffer pH 6.8 exhibited wavelength of absorbance maximum at 271.73 nm, 272.90 respectively. This is near to the reported value shown in Table 9. The predicted theoretical λ_{max} involved, the working λ_{max} was decided as 271.73nm in methanol and 272.90 pH 6.8 phosphate buffer. The spectrum of Miconazole nitrate is shown in (Figs. 2 and 4).

In UV spectroscopy study, the maximum wavelength of Miconazole Nitrate in methanol was found to be 271.73 nm & pH 6.8 buffer was 272 .90 nm respectively.

8.1.4.2 Construction of Beers-Lambert's plot

a) Construction of Beers-Lambert's plot Miconazole nitrate in methanol:

Beers-Lambert's plot of Miconazole nitrate was performed in methanol & is shown in Table 10 & its graph in Fig. 3. Beers-Lambert's plot was fond to be linear in the conc. range of 2-12 µg/ml having coefficient of regression value R^2=0.998.

8.1.5 FITR Spectroscopy of Miconazole nitrate

A powdered mixture of Miconazole nitrate and KBr was used to make a sample, and the spectra was acquired using an FTIR spectrophotometer scanning in the wavelength range of 4000-400 cm-1.The FTIR spectrum of Miconazole Nitrate was shown in Fig. 6 and principle peaks of its FTIR spectra is given in Table 12.

Miconazole nitrate's absorption bands are a result of the groups that make up its molecular structure. The existence of absorption bands corresponding to the functional groups present in the Miconazole nitrate structure validates the identification and purity of the Miconazole nitrate sample that was provided.

8.1.6 Differential scanning calorimetric (DSC) studies

DSC thermogram for Miconazole nitrate is shown in the Fig. 7 and Table 13.

8.1.7 Compatibility Study

8.1.7.1 Fourier transform infra-red spectroscopy

The FTIR Spectra of Miconazole nitrate and Chitosan shown in Fig. 8 and Identification of Functional group in FTIR spectra of Drug and Chitosan in Table 14.

The FTIR Spectra of Miconazole nitrate and PVA shown in Fig. 9 and Identification of Functional group in FTIR spectra of Drug and PVA shown in Table 15.

Physical combination infrared spectra had peaks that matched the drug spectra. The drug's distinctive peaks were also present in the spectrum of all drug-polymer pairings, as illustrated in the graph below (Fig. 10). The drug's significant peaks in the IR spectrum imply that there is no drug-polymer interaction (Table 16).

8.2 Optimization of Miconazole Nitrate Loaded NPs

To study the optimization of Miconazole nitrate loaded NPs, 3^2 randomized full factorial design was selected. Selection of optimize batch is totally based on experimental design lay out In this out of varies quality attribute , % entrapment efficiency and particle size of nanoparticle has been used for optimization process for dependent and independent variables are having very important role. In this study, the amounts of Chitosan (x1) and DCM (x2) were chosen as independent variables. These two variables were rated on three levels: higher, middle, and lower, with coding +1, 0 and -1, respectively. X1 levels of 5, 75, and 100 mg were chosen, whereas X2 levels of 2, 4, and 6 ml were chosen. Entrapment efficiency (Y1) and entrapment efficiency (Y2) were the dependent or response variables. Experimental design layout of Miconazole loaded NPs shown in Table 17.

Table 3. Standard Values of Hausner's ratio

Sr. No.	Hausner's Ratio	Type of flow
1	<1.25	Excellent
2	>1.25	Poor

Table 4. Standard Values of Carr's Index

Sr No.	Carr's Index	Type of flow
1	5-16	Excellent
2	12-16	Good
3	18-21	Fair
4	23-25	Poor
5	33-38	Very poor
6	>40	Extremely poor

Table 5. Standard Values of Angle of Repose

Sr. No.	Angle of Repose	Type of Flow
1	<25	Excellent
2	25-30	Good
3	30-40	Passable
4	>40	Very poor

Table 6. Comparison of result of organoleptic characters of drug sample

Identification Test	Observed Result	Reported Standard
Appearance	Microcrystalline Powder	Crystalline or microcrystalline powder
Colour	White	White to yellowish white
Odour	Odourless	Odourless

Table 7. Melting point of Miconazole nitrate against reference value

Melting Point (°C)	
Reference	**Observed**
175-185°C	181°C

Table 8. Result of solubility study

Solvent	Observed Result(mg/ml)	Standard Result(mg/ml)	Inference
Distilled water	Practically insoluble	Practically insoluble	Practically insoluble
Ethanol	2.9±0.2	3	Poorly soluble
Methanol	11.9±0.6	13	Sparingly soluble
Phosphate buffer pH6.8	11.15±0.8	12	Sparingly soluble

Table 9. Maximum Wavelength (λmax) of Miconazole nitrate in Methanol And 6.8 Phosphate Buffer

Solvent	λmax (nm)	
	Observed	Reported
Methanol	271.73	272
pH 6.8 Phosphate buffer	272. 90	272

Table 10. Absorbance value for different concentration Miconazole Nitrate in Methanol

Sr. no	Concentration (µg/ml)	Absorbance
1	2	0.089
2	4	0.160
3	6	0.231
4	8	0.306
5	10	0.377
6	12	0.456

Table 11. Absorbance value for different concentration Miconazole nitrate in pH 6.8Buffer

Sr. No.	Concentration (µg/ml)	Absorban ce
1	2	0.0065
2	4	0.0135
3	6	0.0201
4	8	0.0251
5	10	0.0326

Table 12. Major peaks observed in FTIR spectrum of Miconazole nitrate.

Sr. No.	Functional group	Standard frequency range(cm^{-1})	Observed frequency (cm^{-1})
1	Imidazole C-N stretching	3140-3250	3182.93
2	Aromatic C-H stretching	3000-3100	3104.83
3	Aliphatic C-H stretching	2850-3000	2351.77
4	C=C aromatic	1450-1590	1579.41
6	C-Cl halogen attached at benzene ring	650-900	816.70
5	Ether C-O group	1490-1680	1554.34

Table 13. Observation table of DSC

Sr. no	Melting point	Standard Melting point	Infere nce
1	182.90°C	175 – 185°C	Sharp endothermic peak was observed

Table 14. Identification of Functional group in FTIR spectra of Drug and Chitosan

Functional Group	Observed Ranges cm-1	Standard Ranges cm-1
C -H Aromatic Stretching	3104	3150- 3050
C=C Aromatic Stretching	1584	1600
N - H (Amine) Stretching	1544	1640 -1550
C – N stretching	1322	1350-1000
C-O Stretching	1008	1300-1000
C-Cl blending	634	785-540

Table 15. Identification of Functional group in FTIR spectra of Drug and PVA

Functional Group	Observed Ranges cm-1	Standard Ranges cm-1
C -H Aromatic Stretching	3104	3150- 3050
C=C Aromatic Stretching	1589	1587
C-N (Amine) Stretching	1322	1350 -1000
C-O Stretching	1284	1300-1000
C-Cl Stretching	757	785-540

Table 16.

Sr. no.	Functional group	Peaks		
		Pure Drug	Pure Drug+ Chitosan +PVA+DCM	Stranded Frequency cm^{-1}
1	C-H Alkane	Observed	Observed	3000-2850
2	C-H (Aromatic)	Observed	Observed	3100-3000
4	C=C (stretch)	Observed	Observed	1680- 1620
5	C-N(Amine)	Observed	Observed	1360-1080
6	C-O (ether)	Observed	Observed	1300-1000
7	C-Cl (Halogens)	Observed	Observed	900-650

Table 17. Experimental design layout of Miconazole loaded NPs

Formulation code	Factor X 1 Chitosan (mg)	Factor X2 Dichloromethane (ml)	Drug entrapment(%) Y1	Particle size (nm) Y2
F1	+1	+1	83.40 %	259.1±0.88
F2	+1	0	77.20 %	271.3±0.14
F3	+1	-1	77.60 %	268.9±0.31
F4	0	+1	89.60 %	248.2±1.2
F5	0	0	93.28 %	234.8±0.72
F6	0	-1	90.36 %	245.5±1.2
F7	-1	+1	84.44 %	256.8±0.97
F8	-1	0	72.40 %	277.4±1.6
F9	-1	-1	80.00 %	260.6±1.45

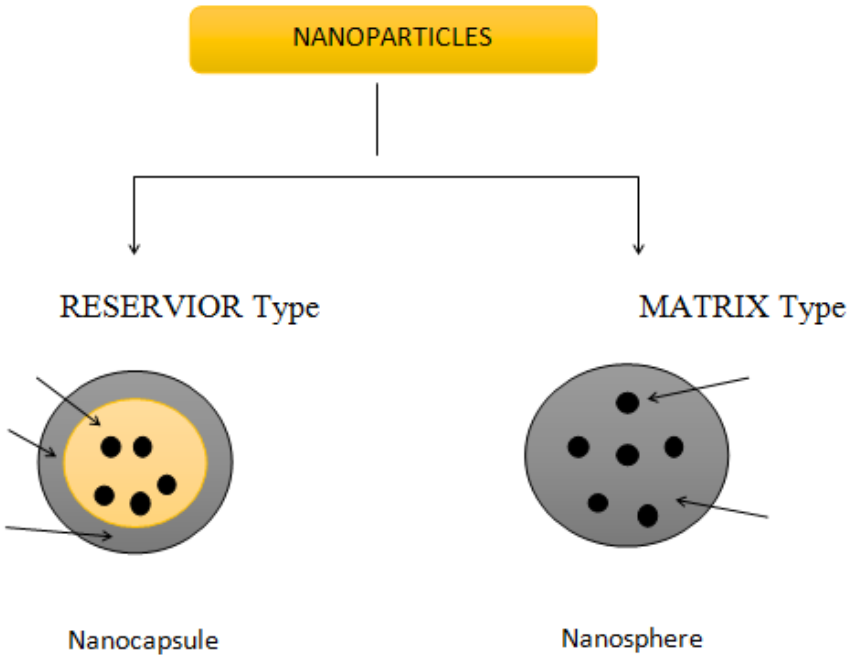

Fig. 1. Types of nanoparticles

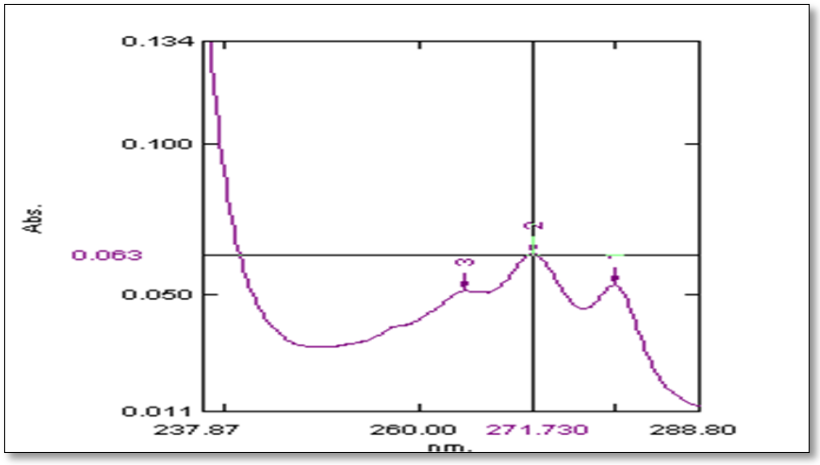

Fig. 2. UV-visible spectrum of Miconazole nitrate in methanol

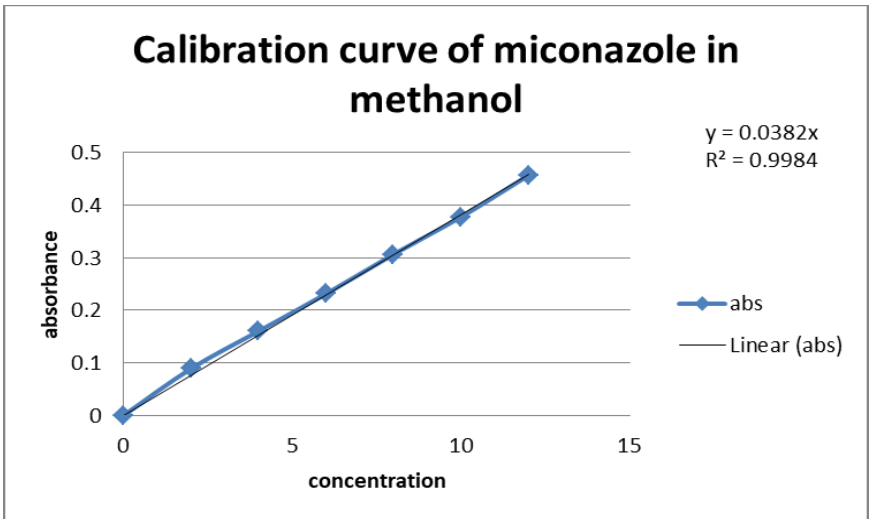

Fig. 3. Calibration curve of Miconazole nitrate in methanol

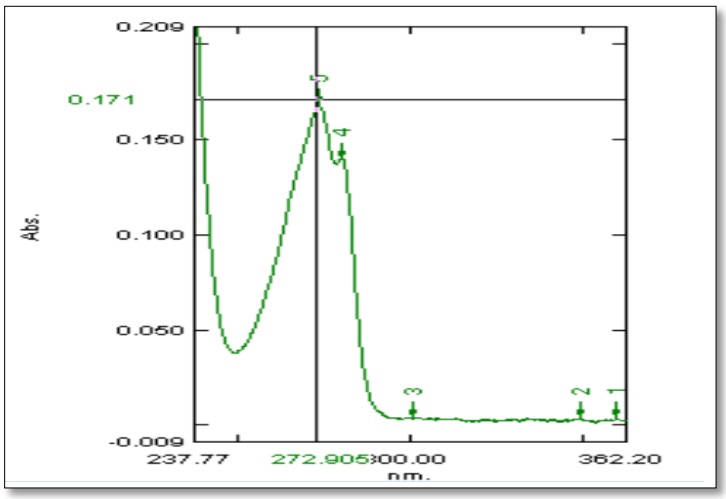

Fig. 4. UV-visible spectrum of Miconazole nitrate in 6.8 phosphate buffer

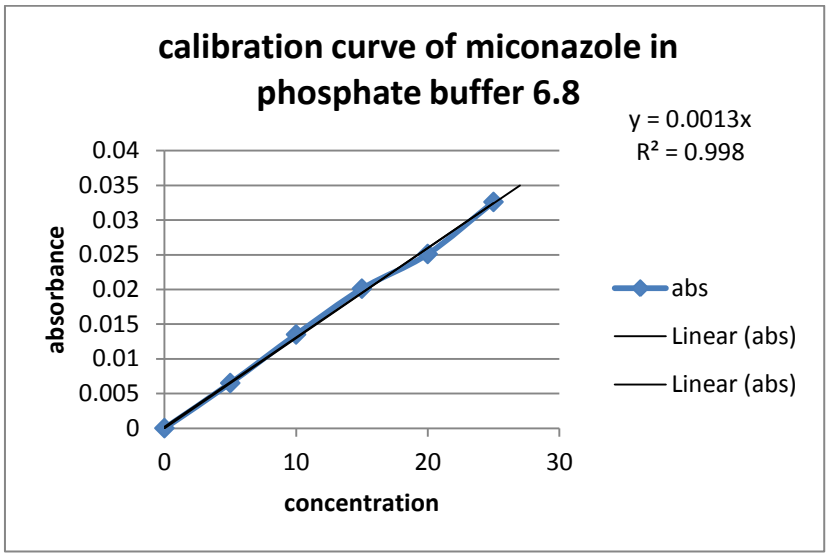

Fig. 5. Calibration curve of Miconazole nitrate in 6.8 phosphate buffer

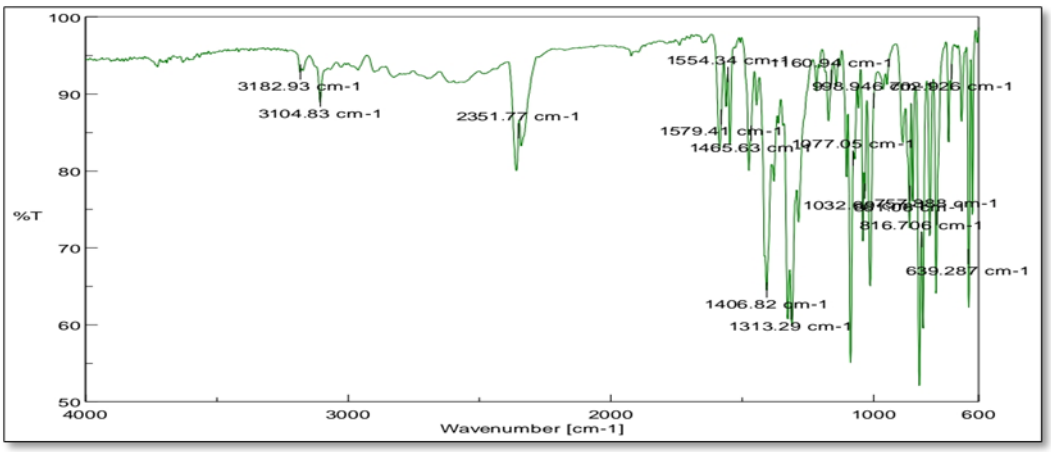

Fig. 6. FTIR spectrum of Miconazole nitrate

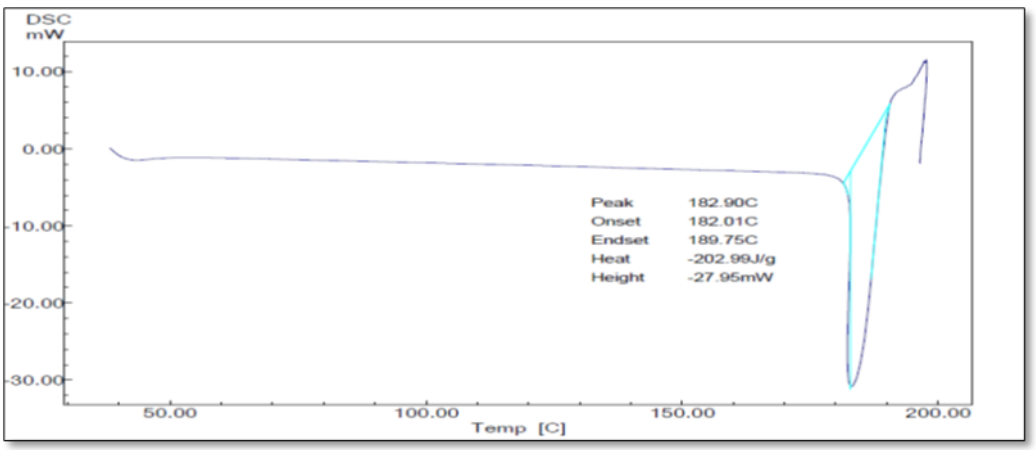

Fig. 7. DSC Themogram of Miconazole nitrate

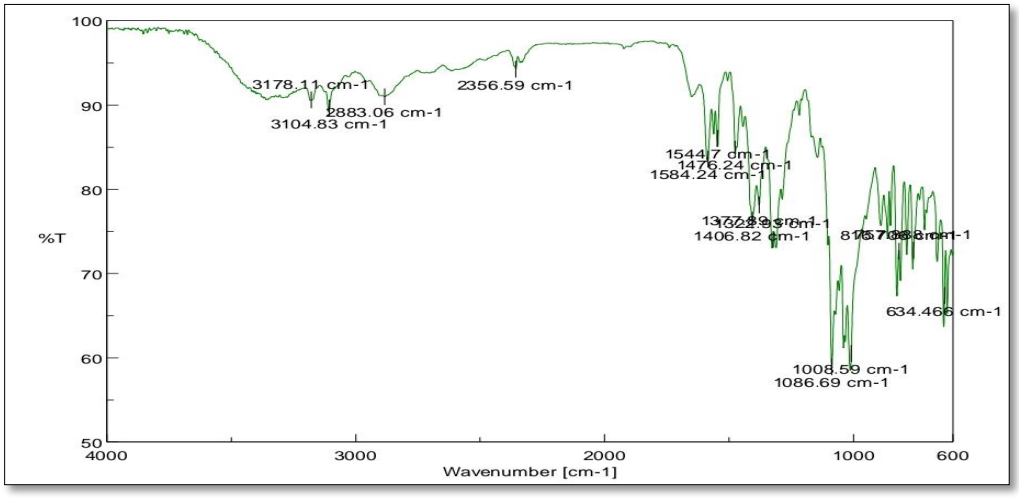

Fig. 8. FTIR Spectra of Miconazole nitrate and Chitosan

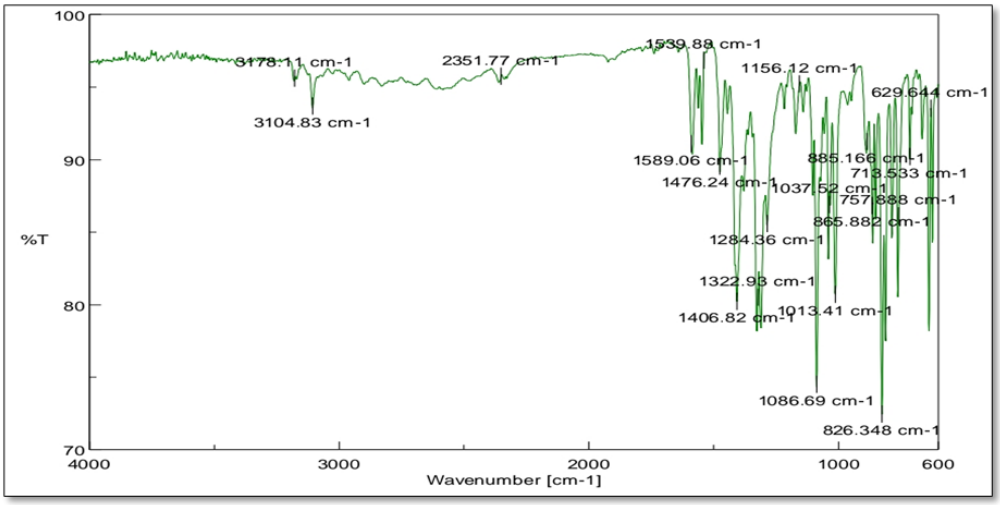

Fig. 9. FTIR spectra of Miconazole nitrate and PVA

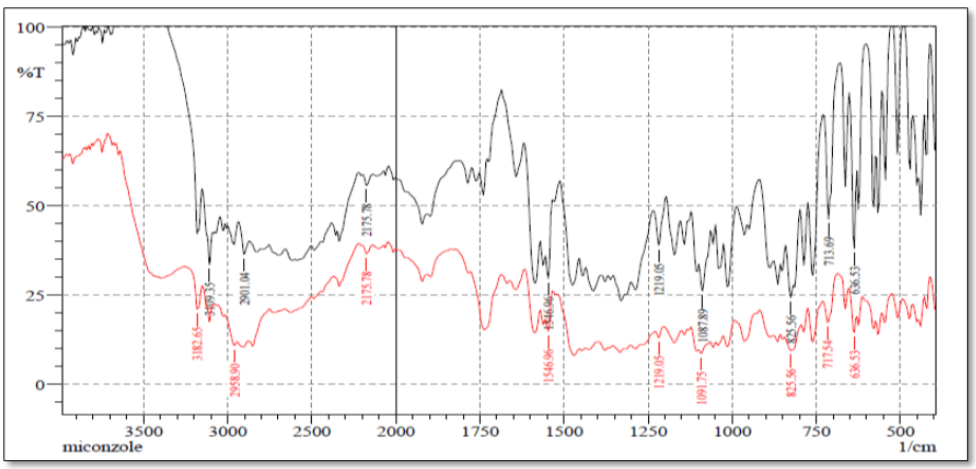

Fig. 10. Infra-red spectrum of drug with polymers

8.3 Optimization of Drug and Polymer

In this study, the amounts of Chitosan (x1) and DCM (x2) were chosen as independent variables. These two variables were rated on three levels: higher, middle, and lower, with coding +1, 0 and -1, respectively. X1 levels of 5, 75, and 100 mg were chosen, whereas X2 levels of 2, 4, and 6 ml were chosen. Entrapment efficiency (Y1) and entrapment efficiency (Y2) were the dependent or response variables. The different batches were evaluated for the appropriate concentration of Chitosan and DCM from these, it is observed that the separately prepared concentration of Drug: Chitosan, Drug: DCM in PVA were formed the more proper nanoparticle respectively. Percentage Entrapment efficiency for drug strength shown in Table 18.

8.4 Micromeritic Parameter of Miconazolr Nanoparticle

Bulk Density:

The bulk density of the F1 to F9 batches ranged from 0.48 to 0.76 gm/ml. Table 19 shows the total value of all batches.

Tapped density:

The tapped density of the F1 through F9 batches ranged between 0.55 and 0.91 gm/ml. Table 19 shows the total value of all batches.

Hausner's ratio:

The Hausner's ratio of F1 to F9 was found to be 1.13 to 1.20, indicating that the nanoparticle's flow characteristics were determined to be outstanding. Table 19 shows the total value of all batches.

Carr's index:

Carr's index of F1 through F9 batches was found to be in the range of 11.87% to 17.14%, that indicate flow property of nanoparticle was found to be excellent and batch F6 shows very poor flow property. Value of all batches is in following Table 19.

Angle of repose:

Angles of repose of F1 to F9 batches were measured in the range of 22.68° to 30.79° that indicate flow property of nanoparticle was found to be good. Value of all batches is in following Table 19.

8.5 Evaluation of Nanoparticle of Miconazole

8.5.1 Physical appearance

Physical appearances of prepared nanoparticles are observed visually. It is actual white crystalline particle having a fine particle size with excellent flow ability.

8.5.2 Production yield

F1 to F9 batches had a wide range of percentage production yields, ranging from 74.46 percent to 92.56 percent. This F5 batch has a high percentage of manufacturing yield of 92.56 percent. It was discovered that Chitosan concentration and Stabilizer time have an impact on nanoparticle manufacturing yield. Due to changes in polymer concentration, the production yield may vary. Table 20 shows the % manufacturing yield of nine batches of nanoparticles.

8.5.3 Entrapment efficiency

Percentage Batches F1 through F9 had entrapment efficiency ranging from 72.40 percent to 93.28 percent. In the F5 batch, the highest percent entrapment efficiency was 93.28 percent, as indicated in Table 20.

8.6 Selection of Optimized Batch

The appropriate concentrations of drug and polymer in the various batches were determined. The batch was optimized on basis of entrapment efficiency, Particles size and F5 batch was selected. From these, it was observed that maximum EE% 93.28 % and Particle size was 234.8.

8.6.1 Lyophilization of nanoparticles

During storage, most NPs formulations demonstrate an increase in particle size in a short period of time. It only has a short shelf life. As a result, lyophilization is essential because it provides chemical and physical stability by avoiding Ostwald ripening and hydrolysis processes. The water replacement hypothesis has been proposed as a mechanism for

nanoparticle stability. At the end of the drying process, hydrogen bonds are generated between cryoprotectants and polar groups on the surface of nanoparticles during lyophilization. By acting as water substitutes, these cryoprotectants help to preserve the native structures of NPs. Because NPs and cryoprotectants are amorphous, maximum H-banding between NPs and stabilizer molecules is possible.

N indicates that batches failed to produce NPs.

It was observed that after addition of cryoprotectants there is slight increase in particles size due to formation of cryoprotectant layer around NPs. From above data 5% W/V of mannitol was selected among other cryoprotectants. Influence of various cryoprotectants and their concentration on particle size shown in Table 21.

8.7 Characterization of Optimized Nanoparticle

The developed batches were subjected to Production yield, Entrapment efficiency, and drug content study. From the various batches developed, nanoparticle prepared by using Polymer and stabilizer were found to be best batch in terms of various evaluation parameters. The following characteristics were used to characterise the optimal ratio F5.

8.7.1 Fourier transform infrared spectroscopy (FTIR)

The FTIR tests are carried out to characterize the drug and to look for any interactions between the drug and the polymers in the formulation. An FTIR analysis of the improve shows the FTIR spectra of a nanoparticle that has been tuned. Within the nanoparticle, the FTIR spectra clearly show no interaction between excipients and drug. The optimized nanoparticle's spectrum was found to be identical to that of pure Miconazole. The developed formulation's FT-IR spectra revealed considerable alterations in the finger print region, which ranges from 600 to 1500 cm-1. This proved that the excipients and Miconazole had formed a connection. Cross connecting causes a major change in the down shift and up shift in the formulation, as evidenced in conditions like S-O and C-N stretching. As a result, it can be stated that there is no significant chemical interaction between the medicine and the carrier. Fig. 11 shows the FTIR spectrum of the optimized formulation, whereas Table 22 shows the FTIR spectrum of miconazole nanoparticle batch F5.

8.7.2 Drug loading

From the NPs formulation; 1ml aliquot was withdrawn accurately, then diluted suitably with methanol and centrifuge at 5000rpm for 15min and then filtered (0.45µm). A UV Visible spectrophotometer set to wavelength 272 nm was used to determine the concentration of Miconazole in the filtrate. The Miconazole content of optimized NPs was found to 86.64%.

8.7.3 Particle size and Poly dispersibility index (PDI)

The Malvern zeta sizer of optimised batch F5 was used to size the particles. The particle size rose in order as the polymer concentration increased, however beyond a specific concentration, the ratio of drug to polymer was increased, and the particle size decreased. Because of the high drug to polymer ratio, the amount of polymer accessible was limited. As a result, it was determined that particle size varied with drug polymer ratio concentration. Table 24 shows the average particle size of the optimised batch F5. It was discovered that the polymer and stabiliser have a substantial impact on nanoparticle particle size. Fig. 12 shows a bar graph of particle size for a developed nanoparticle formulation.

Poly dispersibility index: (PDI):

The particle size distribution index (PDI) measures the width, spread, or variance of the particle size distribution. A lower PDI value implies a monodisperse sample, whereas a higher PDI value indicates a polydisperse sample with a wider particle size variation. The equation PDI=d/davg can be used to determine PDI. In the particle size data sheet, dis is the width of the distribution denoted by SD, while davg.is the average particle size denoted by MV (nm).

$$PDI = \Delta d/davg = 0.4$$

The type of nanoparticle formulation for the optimized batch is Mid-Range monodisperse, as shown in Table 19. Table 23 shows the polydispersity indices of nanoparticles. As a result, the polymer-based nanoparticles generated using the solvent evaporation

approach have a homogeneous size distribution.

8.7.4 Zeta potential

The zeta potential indicates the type of charge present on the nanoparticle's surface as well as the formulation's stability. Electrokinetic potential in colloidal dispersions is a scientific phrase. It's the electric potential difference between the dispersion medium and the stationary layer of fluid associated to the dispersed particle in an interfacial double layer, or the potential difference between the dispersion medium and the stationary layer of fluid attached to the dispersed particle. It's utilised to calculate the charge's magnitude.

Zeta potential graph is shown in the Fig. 13. The zeta potential of optimized batch are shown in Table 25.

8.7.5 Scanning electron microscopy (SEM)

The surface morphology of drug particles can be investigated using scanning electron microscopy (SEM). The image confirms that nanoparticles were spherical in shape, size, and surface structure of nanoparticles, as well as a porous surface with no drug crystal on the surface of nanoparticles, based on SEM photographs of optimised batch F5. The encapsulation has an impact on the size. At 5 KX magnetic resonance, the sample was studied under scanning electron microscopy. Fig. 14 shows the SEM of an optimised F5 formulation.

8.7.6 Differential scanning electron microscopy (DSC)

DSC was also used to investigate the drug-polymer interaction. The DSC thermogram of pure drug reveals a prominent endothermic peak at 182.90°C, which corresponds to the drug's melting point. The endothermic peak of the optimised nanoparticle is slightly different from that of the pure drug in DSC spectra, while the peak strength is significantly lowered. This impact could be due to the drug's crystalline size shrinking. The widening of the peak in the spectra indicates that the medication is largely encased in nanoparticles. F5 had a large endothermic peak on the DSC thermogram at 161.69 0C shown in (Table 26) and Fig. 15.

Table 18. Percentage Entrapment efficiency for drug strength

Formulation Code	Drug Entrapment
F1	83.40 % ±0.87
F2	77.20%±1.23
F3	77.60 %±0.84
F4	89.60 %±0.95
F5	93.28 %±1.45
F6	90.36 %±0.83
F7	84.44 %±1.65
F8	72.40 %±1.907
F9	80.00%±1.24

Table 19. Flow properties parameters of Miconazole loaded nanoparticle

Formulation Code	Bulk Density (gm/ml)	Tapped Density (gm/ml)	Hausner's ratio	Carr's Index (%)	Angle of Repose (°)
F1	0.63±0.08	0.78±0.08	1.20	16.01±0.03	26.73±0.05
F2	0.76±0.04	0.91±0.01	1.23	15.00±0.01	28.05±0.03
F3	0.48±0.03	0.55±0.04	1.14	12.72±0.04	23.31±0.07
F4	0.55±0.01	0.61±0.03	1.18	15.38±0.01	29.24±0.01
F5	0.52±0.03	0.58±0.03	1.13	11.87±0.04	22.68±0.02
F6	0.56±0.06	0.65±0.03	1.17	15.19±0.06	27.15±0.05
F7	0.50±0.09	0.58±0.01	1.16	12.19±0.05	26.61±0.04
F8	0.58±0.04	0.70±0.03	1.20	17.14±0.06	28.50±0.08
F9	0.52±0.06	0.60±0.02	1.15	13.33±0.07	30.79±0.03

Table 20. Production yield, and entrapment efficiency, of Miconazole Nanoparticle

Formulation Code	% Production Yield	% Entrapment Efficiency
F1	84.41±0.13	83.40 %
F2	77.74±0.03	77.20 %
F3	78.54±0.13	77.60 %
F4	85.69±0.02	89.60 %
F5	92.56±0.13	93.28 %
F6	88.53±0.01	90.36 %
F7	84.78±0.04	84.44 %
F8	74.46±0.47	72.40 %
F9	81.73±0.12	80.00 %

Table 21. Influence of various cryoprotectants and their concentration on particle size

Concentration (%W/V)	Particle size (nm) of cryoprotectants				
	Sucrose	Mannitol	Lactose	fructose	dextrose
3%	N	**N**	N	N	N
5%	191.32	**161.31**	170.02	182.81	174.44
7%	248.29	**210.42**	215.84	257.19	220.67

Table 22. FTIR spectrum of miconazole nanoparticle batch F5

Functional Group	Observed Ranges cm-1	Standard Ranges cm-1
C -H Aromatic Stretching	3107	3150 – 3050
C- O stretching	1734	1750 – 1730
C=C stretching	1587	1600
N -H (Amine) blending	1560	1640 – 1550
C -Cl (Halogen) Stretching	761	785 -540

Table 23. Polydispersibility index according to its type of dispersion

Polydispersity index	Type of dispersity
0-0.05	Monodisperse Standard
0.05-0.08	Nearly Monodisperse
0.08-0.7	Mid- Range mono disperse
> 0.7	Very Polydisperse

Table 24. Particle size and Polydispersibility index

Formulation Code	Particle size	Polydispersibility index
F5	234.8 d.nm	0.355

Table 25. Zeta Potential determination of optimized F5 formulation

Formulation Code	Zeta Potential	Conductivity (mS/cm)
F5	3.48	0.0673

Table 26. DSC observation table of Optimized F5 formulation

Sr. No	Melting point	Inference
Pure drug	182.90	Sharp peak indicates purity of drug
Physical mixture	161.69	Broadening of peak observed due to capsulation of drug in vesicles

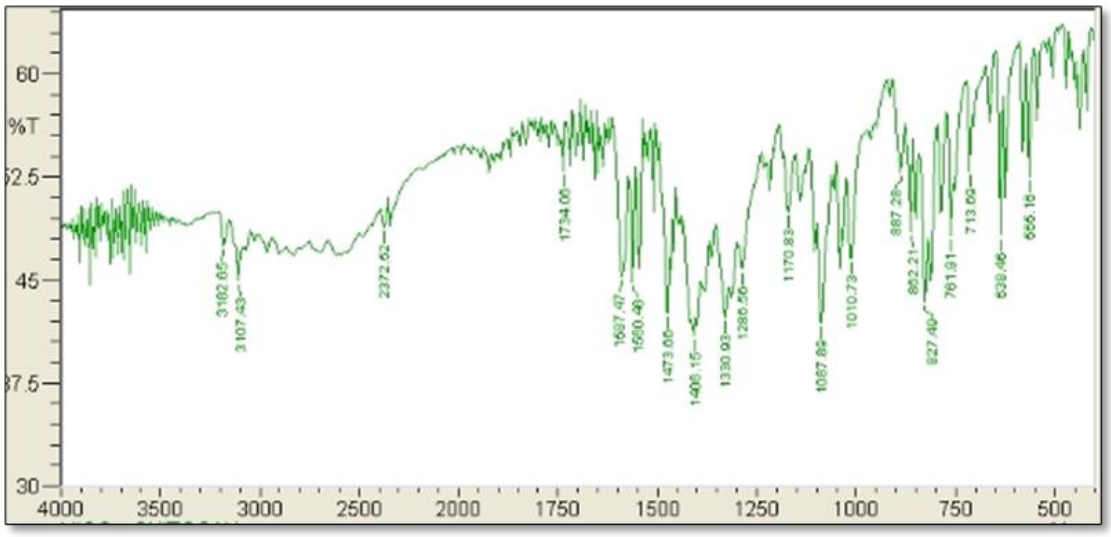

Fig. 11. FTIR of Optimized formulation

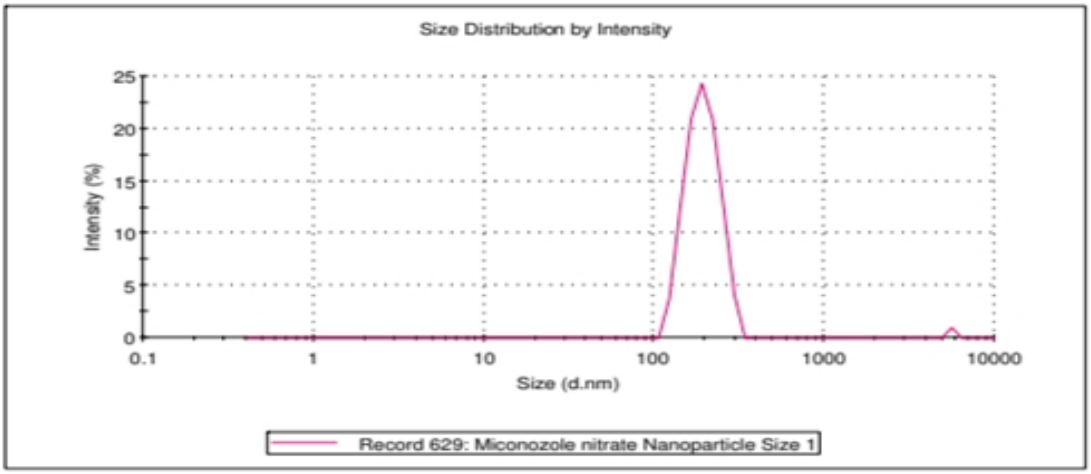

Fig. 12. Particle size of optimised F5 formulation

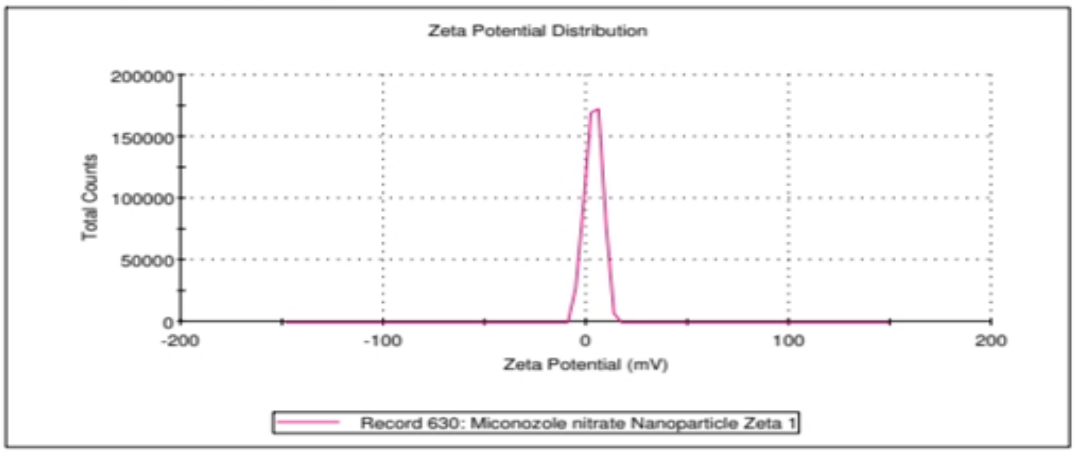

Fig. 13. Zeta potential of optimized F5 formulation

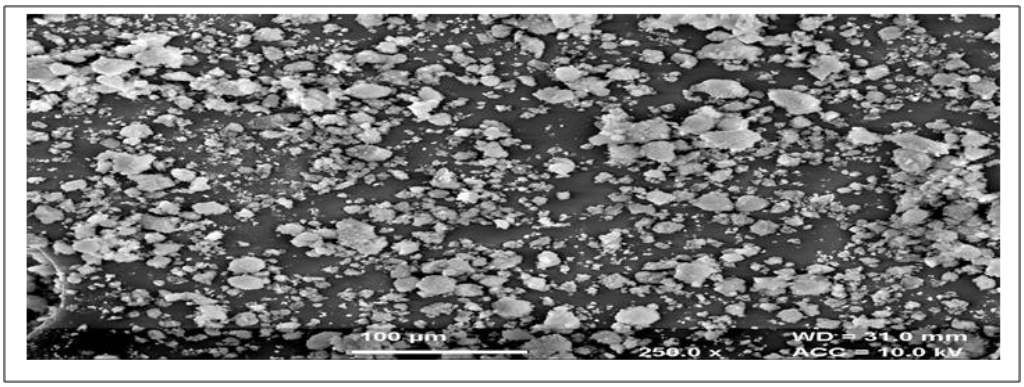

Fig. 14. SEM of optimized F5 formulation

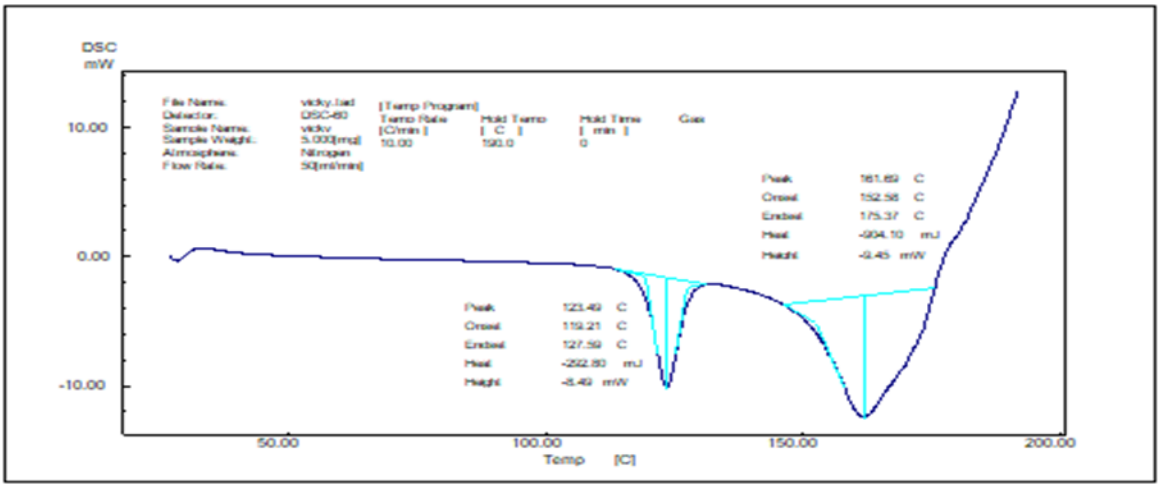

Fig. 15. DSC of Optimized F5 formulation

9. CONCLUSION

From all observations and results obtained, it can be concluded that, NPs of Miconazole has been successfully developed using Emulsification / solvent evaporation method. All the prepared formulation shows satisfied organoleptic properties. As no uncountable peaks were observed in FT-IR analysis, so it confirmed the purity of developed formulation and no interaction of excipients with drug. The Emulsification and Solvent Evaporation method was found to be an effective way for successfully incorporating the medication Miconazole with a high entrapment efficiency. Furthermore, it is possible that obtaining particles in the nanometer range would boost bioavailability. The result obtained from response of experiment it was confirmed that, the formulation F5 in NPs was optimized as they meet all specifications for bulk density, tapped density, Angle of repose, Carr's index, Hausner's ratio, entrapment efficiency, drug content, SEM, Zeta potentiomety and Particle size determination. SEM photographs showed spherical structure having porous surface. Particle size was observed as 234.8 nm of optimized batch F5. The entrapment efficiency of optimized batch was found to be 93.28%. The drug excipient compatibility study for one month at 50ºC /75% RH did not show any changes in the physical properties. The stability study of the drug show no changes in the physical appearance, entrapment efficiency. Nanoparticle gel prepared and evaluated for viscosity, Spredability of nanoparticle gel and results are obtained, which shows nanoparticle formulation shows superior to the marketed conventional gel in the treatment of skin infection such as athletes foot, jock itch , ringworm , and fungal skin infection (candidiasis). Optimized gel formulation was examined for visual appearance and it was found to be transparent. The pH of the formulation was found to be in between the skin pH range which is in tolerable range for

transdermal route. Hence it is concluded that above formulation can be more effective than conventional gel used in athletes foot, jock itch, ringworm, and fungal skin infection (candidiasis).

DISCLAIMER

The products used for this research are commonly and predominantly use products in our area of research and country. There is absolutely no conflict of interest between the authors and producers of the products because we do not intend to use these products as an avenue for any litigation but for the advancement of knowledge. Also, the research was not funded by the producing company rather it was funded by personal efforts of the authors.

CONSENT

It is not applicable.

ETHICAL APPROVAL

It is not applicable.

COMPETING INTERESTS

Authors have declared that no competing interests exist.

REFERENCES

1. Aboofazel R. Nanotechnology: A new approach in pharmaceutics Kinam Park Alexander Florence. Journal of Controlled Release. 2010;141:263-264.
2. Mishra R, Acharya S, Sahoo SK. Cancer nanotechnology: application of nanotechnology in cancer Therapy. Drug Discovery Today. 2010;15:777-782.
3. Darshana P, Joshi K. Int. J. Pharm. Phytopharmacol. Res. 2012;2(1):60-65.
4. U. S. Environmental Protection Agency: "Module 3: Characteristics of Particles Particle Size Categories". From the EPA Website.
5. Vert Michel, Doi Yoshiharu, Hellwich, Karl-Heinz, Hess Michael, Hodge Philip, Kubisa Przemyslaw, Rinaudo Marguerite, Schué François. "Terminology for biorelated polymers and applications (IUPAC Recommendations 2012)". Pure and Applied Chemistry. 2012;84(2):377–410. DOI: 10.1351/PAC-REC-10-12-04.
6. Chae Seung Yong, Park Myun Kyu, Lee Sang Kyung, Kim Taek Young, Kim Sang Kyu, Lee. Wan In. "Preparation of Size-Controlled TiO 2 Nanoparticles and Derivation of Optically Transparent Photocatalytic Films". Chemistry of Materials. 2003;15(17):3326–3331. DOI: 10.1021/cm030171d.
7. Chae Seung Yong, Park Myun Kyu, Lee Sang Kyung, Kim Taek Young, Kim Sang Kyu, Lee Wan In.. "Preparation of Size-Controlled TiO 2 Nanoparticles and Derivation of Optically Transparent Photocatalytic Films". Chemistry of Materials. 2003;15(17):3326–3331. DOI: 10.1021/cm030171d
8. Jacques Simonis Jean, Koetzee Basson Albertus. "Evaluation of a low-cost ceramic micro-porous filter for elimination of common disease microorganisms". Physics and Chemistry of the Earth, Parts A/B/C. 2011;36(14–15):1129–1134. DOI: 10.1016/j.pce.2011.07.064
9. Silvera Batista CA, Larson RG, Kotov NA. "Nonadditivity of nanoparticle interactions". Science. 2015;350(6257):1242477–1242477. DOI:10.1126/science.1242477. PMID 2645021
10. Cai Wei; Nix William D. Imperfections in Crystalline Solids. Cambridge Core; 2016. DOI:10.1017/cbo9781316389508. ISBN 9781107123137. Retrieved 21 May 2020.
11. Chen Chien-Chun, Zhu Chun, White Edward R, Chiu Chin-Yi, Scott MC, Regan BC, Marks Laurence D, Huang Yu, Miao Jianwei. Three-dimensional imaging of dislocations in a nanoparticle at atomic resolution. Nature. 2013;496(7443): 74–77. Bibcode: 2013Natur.496...74C. DOI: 10.1038/nature12009. PMID 23535594.
12. Guo Dan, Xie Guoxin, Luo Jianbin. "Mechanical properties of nanoparticles: basics and applications". Journal of Physics D: Applied Physics. 2014;47(1): 013001. DOI:10.1088/0022-3727/47/1/013001.
13. Khan Ibrahim, Saeed Khalid, Khan Idrees. "Nanoparticles: Properties, applications and toxicities". Arabian Journal of Chemistry. 2019;12(7):908–931. DOI: 10.1016/j.arabjc.2017.05.011.
14. Carlton CE, Rabenberg L, Ferreira PJ. "On the nucleation of partial dislocations in

nanoparticles". Philosophical Magazine Letters. 2008;88(9–10):715–724.
DOI: 10.1080/09500830802307641.

15. Jump up to: A B Knauer, Andrea; Koehler, J. Michael. "Explanation of the size dependent in-plane optical resonance of triangular silver nanoprisms". Physical Chemistry Chemical Physics. 2016;18 (23):15943–15949.
DOI: 10.1039/c6cp00953k.
PMID 27241479.
16. Mahmoud Badry, Nazrul Huq. Solubility and dissolution enhancement of Tadalafil using self nanoemulsifying drug delivery system. Journal of Olio Science. 2014; 567-576.
17. Available:http://en.m.wikipedia.org/wiki/Tadalafil.
18. Muller RH, Mader K. Solid Lipid Nanoparticles for Controlled Drug Delivery- A Review of the State of the art", European Journal Pharm Bio Pharm. 2000;50(1): 161-177.
19. Mahmoud Badry, Nazrul Huq. Solubility and dissolution enhancement of Tadalafil using self nanoemulsifying drug delivery system. Journal of Olio Science. 2014; 567-576.
20. Chatwal G, Anand S. Instrumental method of chemical analysis. 5th Edition. Himalaya Publishing House. 2008;2.149-2.184, 2.303-2.366.
21. Brahmankar DM, Jaiswal SB. Biopharmaceutics & Pharmacokinetics a treatise. 1st edition, Delhi, Vallabh Prakashan. 2003;335-71.
22. Skoog H. Instrumental analysis. Cengage Learning Publication. 2007;478-599.
23. Sajid khan Sadozai, Saeed Ahmad Khan, Nasiara Karim, Dennis Becker, Nils Steinbruck, Stefanie Gier, Abdul Baseer, et al. Ketoconazole loaded nanoparticlr and its synergism against *Candida albicans* when combined with silver nanoparticle. Journal of Drug Delivery Science and Technology; 2020.
DOI: https: //doi.org/10.1016/j.jddst.2020 . 101574.
24. Donald L. Pavia, Gary M. Lampman, George, S. Infrared Spectroscopy. 2009;38-39.
25. Chatwal G, Anand S. Instrumental method of chemical analysis. 5th edition. Himalaya Publishing House. 2008.2.149-2.184, 2.303-2.366.
26. Rahul Nair, Arun Kumar KS, Vishnu Priya K, Sevukarajan M. Recent Advances in Solid Lipid Nanoparticle Based Drug Delivery Systems. J Biomed Sci and Res. 2011;3(2):368-384.
27. Salomy M, Gautami J. Design and Evaluation of Topical Formulation of Diclofenac Sodium for Improved Therapy. International Journal of Pharmaceutical Sciences and Research (2015); 1973.
28. Madhshri M, Thakur RS. Formulation and evaluation of solid lipid nanoparticles containing clotrimazol. American Journal of Pharmtech Research. 2012;2(3):536-550. ISSN: 2249-3387.
29. Osmani M, Rohit R. Bhosale. Nanosponges: The Spankling Accession in Drug Delivery- An Updated Comprehensive Review. Pelagia Research Library. 2014;5(6):7-21.
30. Bolten S, Bon C. Pharmaceutical Statics Practical and Clinical Applications. 4th edition revised and expanded, Marcel Dekker. 2004;135:265-288.
31. Rathopan A, Sven-lverlorenzen, and Sunee S. Effect of solid lipid nanoparticles Formulation composition on their size, zeta potential and potential for in vitro pHIS-HIV-Hugag Transfection. Pharmaceutical Research. 2007;6(24):1098-1107.

Peer-review history:
The peer review history for this paper can be accessed here:
https://www.sdiarticle4.com/review-history/73307